(A New Proposal to Jefferson Lab PAC-21)

A Search for Neutral Baryon Resonances Below Pion Threshold

F. Benmokhtar, C. Glashausser, R. Gilman, X. Jiang (Co-spokesperson)[a], G. Kumbartzki, R. Ransome (Co-spokesperson)

Rutgers University, Piscataway, New Jersey.

J.-P. Chen, E. Chudakov, L. Elouadrhiri, D.W. Higinbotham, M. Jones, J. LeRose, D. Mack, R. Michaels, S. Nanda, B. Reitz, A. Saha, W. Wojtsekhowski

Jefferson Lab, Newport News, Virginia.

D. Margaziotis

California State University, Los Angeles.

P. Markowitz

Florida International University, Miami, Florida.

T.-H. Chang

University of Illinois, Urbana-Champaign, Illinois.

G. Chang, J. Kelly

University of Maryland, College Park, Maryland.

G. A. Peterson

University of Massachusetts at Amherst, Amherst, Massachusetts.

J. Calarco

University of New Hampshire, Durham, New Hampshire.

Abstract: Possible evidence for neutral baryon resonances at 1004, 1044, and 1094 MeV were reported in pp inelastic scattering data in 1997. We propose using the Hall-A high resolution spectrometer pair to perform coincident $p(e,e'\pi^+)X^0$ measurements with missing mass resolution of 0.5 MeV. We seek to observe abnormal structures in the missing mass spectra in the mass region of $m_N \leq m_{X^0} \leq m_N + m_\pi$. A confirmation of such a structure will raise serious challenges to the existing framework of the quark model. A null result will directly contradict the published evidence, and set a tight upper limit of $\sigma_{p(e,e'\pi^+)X^0}/\sigma_{p(e,e'\pi^+)n} \leq 1.0 \times 10^{-4}$. A total of 120 hours (5 days) of beam time is requested.

[a] Contact person. Email: jiang@jlab.org

1 Physics Motivation

Since the discovery of the $\Delta(1232)$ resonance in the 1950s, many baryon resonances have been discovered above the mass of the Δ. These baryon states are interpreted in the quark model as net three-quark color-singlet objects with angular and radial excitations [1]. The quark model explains the mass difference of $m_\Delta - m_N$ by quark spin-spin interactions [2]. Since all the low-lying quark-model states are accounted for, a baryon bound state with a mass between the nucleon and the Δ should not exist in the present theoretical framework. Indeed, such a resonance had never been reported prior to 1997, and several searches [3,4] for charge-two resonances yielded null results in this mass region. However, in 1997, a French group published possible evidence for neutral baryon resonances at 1004, 1044, and 1094 MeV in pp inelastic scattering [5]. The strength of these states were of the order of a few parts of 10^{-4} compared to that of the $pp \to p\pi^+ n$ reaction. The existence of such unexpected resonances, if proved to be true, will fundamentally change our understanding of quark-quark interactions.

The experimental results of Ref. 5 are most astounding when one considers the countless experiments carried out with many different probes over more than 50-years in which these resonances were never observed. Serious doubts were raised by experimentalists and theorists alike [8], and plans were extensively discussed at facilities such as MIT-Bates, SAL, and MAMI, to conduct measurements to verify the claims of Ref. 5 using real or virtual photon probes. However, to our knowledge, no data of good quality has been presented to confirm or contradict the published results of Ref. 5.

In this proposal, we directly addresses the question of whether a charge neutral, non-strange, low-mass state with baryon number unity exists. We propose a simple and clean $p(e,e'\pi^+)X^0$ measurement to search for abnormal structures in the reconstructed missing mass spectra, taking full advantage of the high-resolution spectrometer pair in Hall A and the high intensity, high duty-factor CW beam of Jefferson Lab. If positive evidence is found, unexpected physics could emerge. In the case of a null result, strong doubts will be raised about the validity of the published results of Ref. 5, and a tight upper limit of $\sigma_{p(e,e'\pi^+)X^0}/\sigma_{p(e,e'\pi^+)n} \leq 1.0 \times 10^{-4}$ can be set on the existence of such resonances.

A one-shift test run was conducted in Hall A in April of 2001 to serve as a guide for the development of this proposal. From the limited statistics of the test run, we concluded that $\sigma_{p(e,e'\pi^+)X^0}/\sigma_{p(e,e'\pi^+)n} \leq 1.0 \times 10^{-3}$. We will argue in later sections that the planned improvements on scintillator timing and target-cell design in Hall A can improve our sensitivity by one order of magnitude.

We believe that the consequences of a positive signal for the existence of such states, which we will label as "X", could be so striking that they merit a serious search. The lack of theoretical prediction is a strong argument in favor, rather than against, searches of important new effects. If an X particle is found, it will signify that there is new, unknown structure to the nucleon. We claim that very weakly

excited states can only be observed when searched for seriously in dedicated experiments. This usually requires a great deal of care, effort, expenditure and accelerator time, and most of all, very high resolution detectors. Detailed attention must be paid to backgrounds and instrumental effects which can lead to false structures. We believe that if these states exist they are unlikely to be discovered accidentally.

1.1 Could an excited baryon state exist below pion threshold ?

We point out here that the existence of a baryon state below pion threshold cannot be explicitly ruled out in the framework of the quark model, although such a state is not predicted by quark models either. The question of whether such a state could exist was first raised in 1970 by Azimov [6]. It was suggested that such a state could be discovered in the missing mass measurements of pp, πp or ep scattering. Because of quark-number (i.e. baryon number) conservation, the X particles must contain a net number of three quarks (presumably the light quarks u and d). Isospin symmetry, reflecting the small u-d quark mass difference and the electromagnetic interaction, could apply, and similar to the case of ordinary hadrons, we expect an (X^0X^+) doublet and/or a quartet $(X^-X^0X^+X^{++})$. Since the decay $X \to N\pi$ is kinematically forbidden, the only possible decay channel is the radiative one. Therefore, a very narrow physical width, of the order of $\Gamma_X \sim 1$ eV is expected.

The new states, if they exist, should be qualitatively different from the ordinary hadrons, and hence have very small "wave-function" overlaps with ordinary nucleons. This is expected to lead to a suppression of electromagnetic and weak XN transition matrix elements by:

$$\frac{g^2(A)_{XN}}{g^2(A)_{NN}} \approx \frac{g^2(V)_{XN}}{g^2(V)_{NN}} \approx K_{EW}, \tag{1}$$

where the electroweak suppression parameter $K_{EW} < 1$ and $g(A)$ and $g(V)$ are the axial-vector- and vector-current coupling, respectively. A similar suppression should hold for strong transition matrix elements, we define:

$$\frac{g^2_{XN\pi}}{g^2_{NN\pi}} \equiv K_S, \tag{2}$$

and expect that $K_{EW} \approx K_S$ possibly to within one or two orders of magnitude. Alongside the mass m_X, the two suppression parameters K_{EW} and K_S provide the main phenomenological characterization of the X particle. We point out that one cannot establish an explicit argument that $K_{EW} \equiv K_S \equiv 0$ based on first principles. A statement that the "X" particle doesn't exist is only meaningful in terms of experimental upper limits of the suppression parameters K_{EW} and K_S. Different reaction channels are sensitive to different suppression parameters. In this proposal, we are sensitive to K_S for the X^0 particle to the level of $K_S \approx 1.0 \times 10^{-4}$.

The condition that a new nucleon-like pole will not spoil the calculation of $\mathrm{Re}f_{\pi N}(\theta = 0)$, via dispersion relation, leads to a loose upper limit [6,7] of $g^2_{\pi NX} \leq 0.1 g^2_{\pi NN}$. The smallness of the πNX vertex might be a consequence of the sharp

difference in inner quark structure of N and X. From the $\gamma\gamma$ angular correlation in the capture of stopped π^- in hydrogen, an upper limit can be set on the electromagnetic $X\gamma$ coupling. The process of $\pi^- p \to X\gamma \to N\gamma\gamma$ would lead to a $\gamma\gamma$ angular distribution different from that of $\pi^- p \to n\pi^0 \to N\gamma\gamma$. The upper limit was set [6] to $W(X\gamma)/W(N\gamma) \leq 0.001$.

Several experiments have searched for charge-two excited baryon states (X^{++}, $I = 3/2$). The Particle Data Book documents two such searches. The most recent one [3] was conducted at TRIUMF (E544, A. J. Yavin and D. Frekers spokespersons) through the reaction $pp \to X^{++}n$ using magnetic spectrometers as momentum analyzers to detect the X^{++} particles. The existence of a charge-two baryon resonance was ruled out at the level of

$$\frac{\sigma(pp \to nX^{++})}{\sigma(np \to pn)} \leq 7.5 \times 10^{-8} \tag{3}$$

Another search for charge $Z = \pm 2$ and $Z = \pm 5/3$ excited states was carried out at KEK using a 12-GeV proton beam [4]. No candidate event was found in the mass range up to $M/Z = 1.2$ GeV/c^2, and an upper limit was established at the 10^{-9} level on the yield of an excited state relative to the pion yield.

Although the existence of a double-charge excited state was ruled out to better than the 10^{-7} level, the possibility of an X^+ or X^0 excited state was not carefully investigated before Ref. 5. In this proposal we focus our efforts on a search for a neutral baryon state (or states), in the mass region of $m_N \leq m_{X^0} \leq m_N + m_\pi$.

1.2 Possible Evidence From Experiments

In 1997, possible evidence of narrow baryon resonances was reported in pp inelastic scattering data from Saturne [5] (the original paper is attached in the Appendix). Proton beams with energies of 1520, 1805, and 2100 MeV were scattered off a liquid hydrogen target. The scattered proton and pions were detected in a magnetic spectrometer. The missing mass spectra in the $pp \to p\pi^+ X^0$ reaction demonstrated unexpected structures at 1004, 1044, and 1094 MeV. These structures persisted when the proton beam energy and scattering angle were altered. Figure 1 illustrates the reaction channels in the measurement, and Fig. 2 shows the cross sections as functions of missing mass at two different beam energies and three different proton scattering angles.

These structures were clearly above statistical fluctuations, typically by more than four standard deviations. In the most significant case, shown in Fig. 3, a structure at 1004 MeV was identified as being 17 standard deviations above statistical fluctuations. The observed width of these structures were about 4-15 MeV, consistent with the resolution of the apparatus. It was carefully argued that these structures could not result from particle mis-identifications, detector defects, secondary scattering from slits or contributions from the target cell. The strength of these states were of the order of a few parts of 10^{-4} compared to that of the $pp \to p\pi^+ n$ peak.

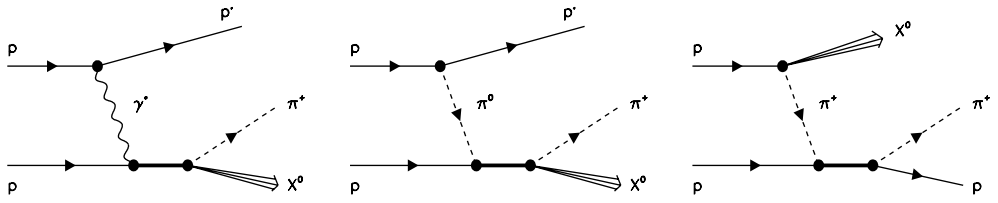

Figure 1: Reaction channels in the $pp \to p\pi^+ X^0$ measurements.

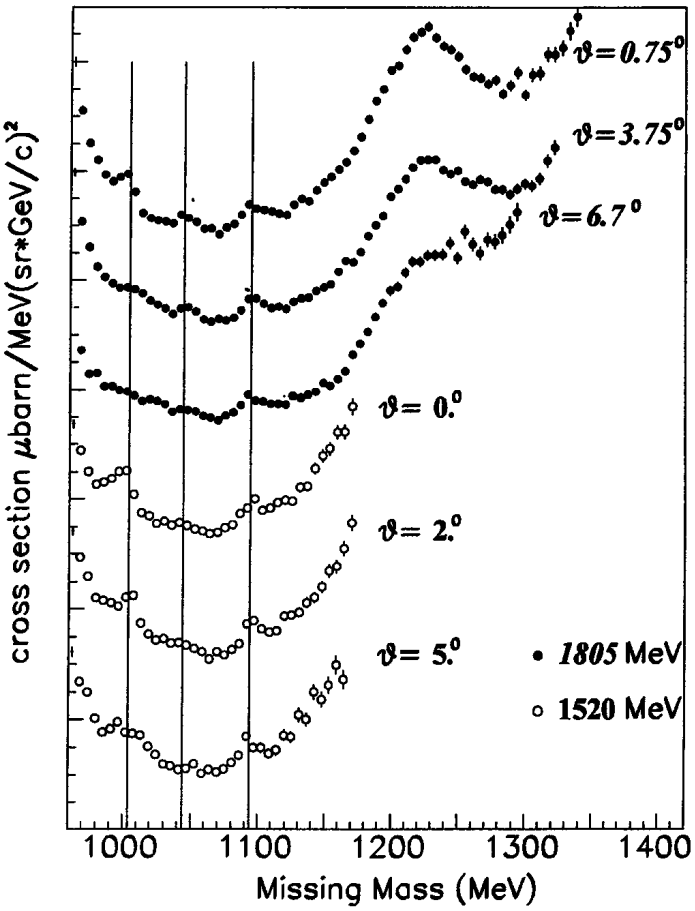

Figure 2: From B. Tatischeff et al. Missing mass differential cross-sections for the $pp \to p\pi^+ X^0$ reaction for the three lowest angles at $T_p = 1520$ and 1805 MeV, selected for missing masses larger than 960 MeV. Data have been binned into 5.6 MeV bins and shifted in the vertical direction in order to fit six angles in the same figure. Individual missing mass plots are attached in the Appendix.

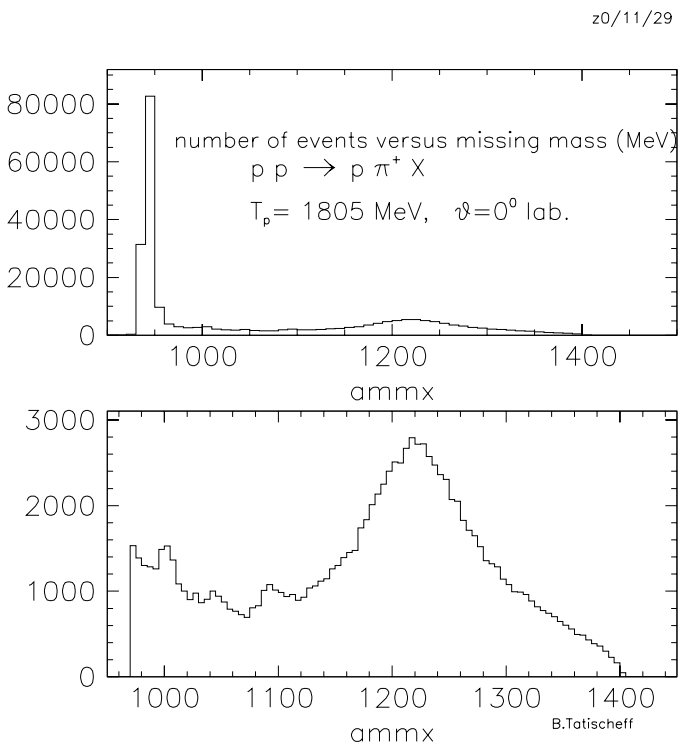

Figure 3: From B. Tatischeff, private communications. Raw missing mass plot of $pp \to p\pi^+ X^0$ at $T_p = 1805$ MeV and $\theta_p = 0°$ without acceptance correction. The horizontal axis indicates missing mass in MeV. Top plot shows the whole spectrum with a narrow neutron peak to the left and a broad Δ^0 bump to the right. The bottom plot shows the region above the nucleon mass.

Since the published evidence of narrow states in the nucleon are very surprising indeed, they meet with considerable skepticism. L'vov and Workman [8] argued that the reported structures are "completely excluded" by the fact that no such structure was reported in the existing real Compton data [9]. As a counter argument, Tatischeff *et al.* [10] pointed out that none of the earlier Compton scattering data were accurate enough to be able to ascertain the presence of new states. Furthermore, it was argued that the overlap between the nucleon and narrow state wave functions might not necessarily be large, thus, a suppressed γp (or γn) channel cannot rule out a narrow state being produced in hadronic excitations or hadronic decays.

Recently, Fil'kov *et al.* published missing mass spectra of the $pd \to ppX_1$ reaction [11] obtained with a 305 MeV proton beam. As shown in Fig. 4, "dibaryon-type" peaks at 1904 ± 2, 1926 ± 2 and 1942 ± 2 MeV in the pX_1 system were claimed. In addition, single baryon peaks at 966, 987, and 1003 MeV were observed in the X_1 mass spectra, and were interpreted as supporting evidence for the narrow baryon resonances of Ref. 5.

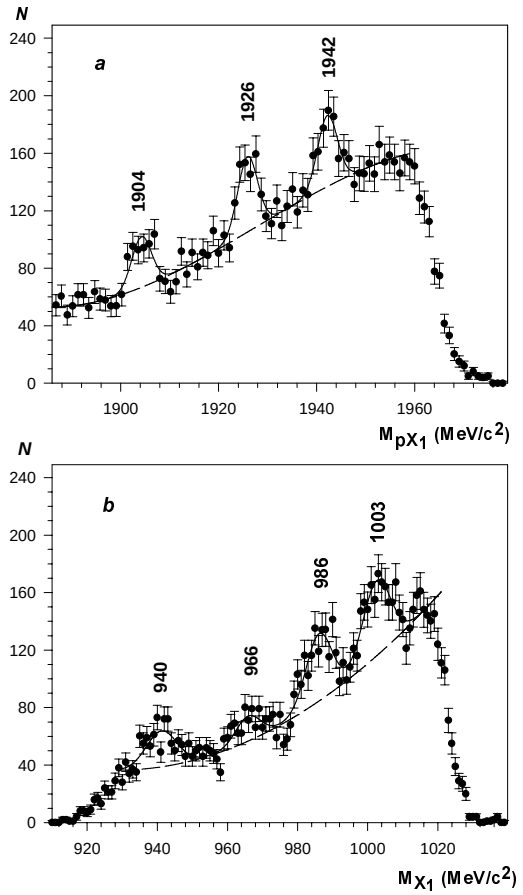

Figure 4: Missing mass plot from Fil'kov *et al.* of the reaction $pd \to ppX_1$. Missing mass M_{pX_1} (a) and M_{X_1} (b) spectra. The dashed and solid curves are results of a fit by polynomials for the background and Gaussians for the peaks, respectively.

1.3 Possible Interpretations of Quark Cluster Model

Colored Quark Clusters

Although it was not proven that these structures were a manifestation of colored quark clusters, a simple model based on the idea of colored quark clusters, such as $(q\bar{q})^2$-q^3 and q^2-q, was presented in the Saturne experimental paper [5]. The mass formula for two clusters of quarks at the end of a stretched bag was derived in terms of color magnetic interactions as [12]:

$$M = M_0 + M_1 \left[i_1(i_1+1) + i_2(i_2+1) + (1/3)s_1(s_1+1) + (1/3)s_2(s_2+1) \right] \qquad (4)$$

where M_0 and M_1 are parameters deduced from mesonic and baryonic mass spectra, and $i_1(i_2)$ and $s_1(s_2)$ are the isospin and spin of the first and the second quark clusters, respectively. The assumption was made that the clusters are q^2-q or $(q\bar{q})^2$-q^3 types. The spin (isospin) values for a diquark $(q\bar{q})$ cluster are 0 or 1, and for a three quark cluster are 1/2 or 3/2. Free parameters were fixed to be $M_0 = 838.2$ MeV and $M_1 = 100.3$ MeV by requiring the mass of nucleon and that of the Roper resonance (1440 MeV) to be reproduced exactly. When all possible spin and isospin configurations were considered, states at 1005 MeV ($S = 1/2$ or $3/2$, $I = 1/2$), 1039 MeV ($S = 3/2$, $I = 1/2$) and 1106 MeV ($S = 1/2$, $3/2$ or $5/2$, $I = 1/2$) were predicted.

Colorless Quark Clusters

Recently, N. Konno [13] pointed out that the masses of these anomalous baryon states can also be well reproduced by the mass formula of the diquark cluster model (DCM) [15] which does not assume colored quark clusters and does not involve any new free parameter.

The DCM model describes a quark system $q^k\bar{q}^h$ in the jj-coupling dominated scheme. The mass formula of such a system consisting of u and d quarks is [14]:

$$\begin{aligned} M = {} & (k+h)m + M\left(1p\frac{1}{2}\right) n\left(1p\frac{1}{2}\right) + M\left(1p\frac{3}{2}\right) n\left(1p\frac{3}{2}\right) \\ & + M\left(1d\frac{3}{2}\right) n\left(1d\frac{3}{2}\right) + M\left(2s\frac{1}{2}\right) n\left(2s\frac{1}{2}\right) + M\left(2p\frac{1}{2}\right) n\left(2p\frac{1}{2}\right) \\ & + \Delta_0\left(n_{\phi_0} + n_{\bar{\phi}_0}\right) + \Delta_1\left(n_{\phi_1} + n_{\bar{\phi}_1}\right) + \sum \Delta_{TS}, \end{aligned} \qquad (5)$$

in which

$$\Delta_0 = a - \frac{3}{4}b, \qquad \Delta_1 = a + \frac{1}{4}b, \qquad (6)$$

where m is the effective mass of u and d quarks, a is the energy that is necessary for the formation of diquark clusters, b is the strength of color-magnetic interaction, $n_{\phi_0}(n_{\bar{\phi}_0})$ and $n_{\phi_1}(n_{\bar{\phi}_1})$ are the numbers of the scalar diquarks (anti-diquarks) ϕ_0 $(\bar{\phi}_0)$ and vector diquarks (anti-diquarks)ϕ_1 $(\bar{\phi}_1)$ involved in the system, respectively. δ_{TS}

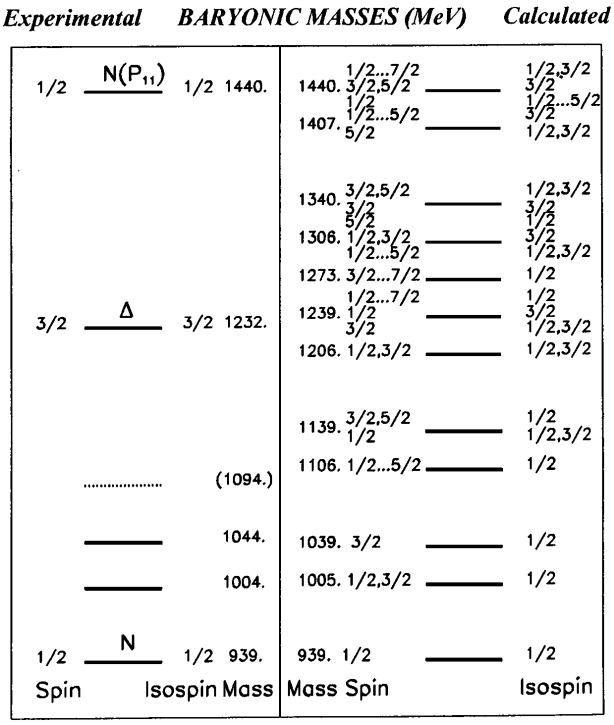

Figure 5: From B. Tatischeff *et al.* Baryonic experimental and calculated masses based on colored quark cluster mass formula.

is the correction energy for the two quarks in the excited diquark with a configuration $[(1p\frac{1}{2})(1s\frac{1}{2})]$ coupled to isospin T and spin S. $M(nlj)$ is the single-particle excitation energy to the shell with principal quantum number n and orbital and total angular momenta l and j, and $n(nlj)$ is the total number of the excited quarks and anti-quarks in the shell. The energy $M(nlj)$ is given by a function of m and angular frequency ω of the binding oscillator potential by:

$$M\left(1p\frac{1}{2}\right) = \omega - \frac{\omega^2}{2m}, \qquad M\left(1d\frac{3}{2}\right) = 2\omega - \frac{3\omega^2}{4m}. \tag{7}$$

All free parameters were fixed ten years earlier[15] using data of baryon masses and the πd phase-shift,

$$m = \omega = 300\ MeV, \quad a = 187\ MeV, \quad b = 195\ MeV,$$

$$\Delta_{00} = \Delta_{11} = 0, \quad \Delta_{10} = -60\ MeV, \quad \Delta_{01} = 10\ MeV.$$

Without introducing colored quark clusters and without any new free parameter, DCM predicted several low-lying resonance states surprisingly close to the observed masses. Figure 6 illustrates the DCM predictions[13].

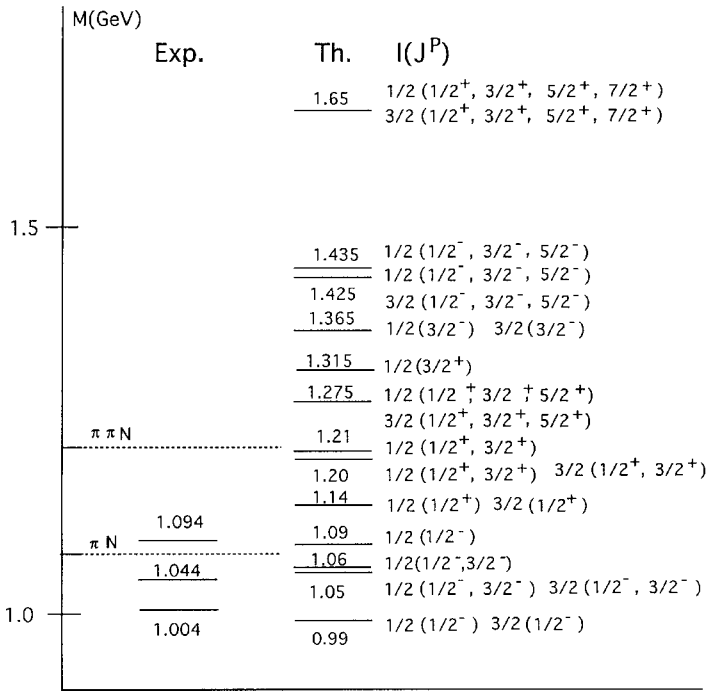

Figure 6: Predicted mass levels from N. Knono's diquark cluster model calculation.

Other Explanations

It was also argued by A. Kobushkin [16] that the claimed narrow baryon resonances could be metastable levels in the quark system as a member of a total antisymmetric representation of the spin-flavor $SU(6)_{SF}$ group. Due to the symmetry of the spin-flavor wave function, they cannot be excited by one photon or decay into the one photon channel. Therefore, their simplest decay channel is two photon decay, $2\gamma N$.

Very recently, it was proposed by T. Walcher [17] that a model based on the excitation of collective states of the quark condensate could explain the narrow baryon resonances as multiple production of a "genuine" Goldstone Boson with a mass of ≈ 20 MeV.

2 The Proposed Measurements

We propose to perform coincident $(e, e'\pi^+)$ measurements with the Hall A high resolution spectrometer pair to study the $p(e, e'\pi^+)X^0$ reaction at $Q^2 = 0.3$ (GeV/c)^2. The invariant mass of the π^+X^0 system $W \approx 1440$ MeV is chosen to closely resemble the kinematics of Ref. 5. As illustrated in Fig. 7, the X^0 state would be a

product of a strong interaction process, and our measurement will be sensitive to the suppression factor K_S. The choice of this reaction has the advantage of closely resemble that of the first diagram of Fig. 1, and we will be searching for the same neutral resonances as claimed in Ref. 5, rather than its charged partner. A missing mass measurement will allow us to take full advantages of the state-of-art Hall A magnetic spectrometers and their high resolution detectors. Compared with a single arm experiment, a coincidence measurement has a much reduced background and can give us better controls on false structures caused by instrumentation flaws.

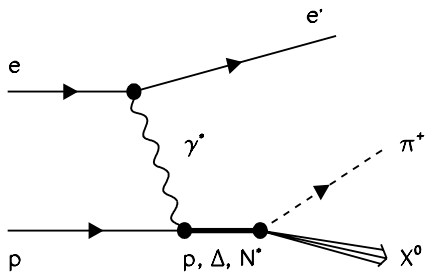

Figure 7: The diagram of the $p(e, e'\pi^+)X^0$ reaction.

2.1 The Choice of Kinematics

The values of W and Q^2 were chosen to match that of Ref. 5. A one-shift test run was conducted to guide the design of this proposal. We chose our kinematics based on the test run.

The kinematics and beam time needed are listed in Table 1. A two-hour calibration run of $p(e, e'\pi^+)n$ measurement is planned to calibrate time-of-flight corrections and check missing mass resolutions. The HRS spectrometers will not be moved throughout the experiment, only the field of the hadron arm will be adjusted. A beam time of 110 hours is planned for the search, which will be split into two parts with the hadron-arm momentum settings altered by 1.0% so that false peaks caused by instrumentation flaws can be eliminated.

Table 1: Table of kinematics and beam time for the proposed measurements.

	E_0 (GeV)	E' (GeV)	ϕ_e	Comments
	1.721	0.990	23.5°	E-arm
	ϕ_π	P_π (GeV/c)	Time (Hours)	H-arm
Kin-A	42.0°	0.659	2.0	$m_{X^0} = m_n$ calibration
Kin-B	42.0°	0.549	110.0	$0.97 < m_{X^0} < 1.07$ GeV

2.2 Experimental apparatus

The challenge of this experiment is to improve the signal-to-noise ratio and to optimize the missing mass resolution. Coincidence time resolution is the key factor governing the signal-to-noise ratio. Precise vertex reconstruction will also help to eliminate accidental events. The missing mass resolution and the vertex resolution can be much improved with a well-designed target cell and direct vacuum couplings between the scattering chamber and the spectrometers.

Spectrometer and detector

The Hall A high resolution spectrometers in their standard detector configuration will be used. The electron arm detector package will include two planes of trigger scintillators, two high resolution tracking VDCs, one gas Cherenkov counter and a double-layered lead-glass shower counter. The particle ID provided by the combination of shower and Cherenkov detectors is more than enough to provide good π^-/e separation for this experiment. In the hadron arm, π^+/p separation at ≈ 600 MeV/c momentum can be independently provided by particle velocity measurements at the focal plane and by scintillator ADC signals. In addition, coincident time-of-flight and vertex cuts are methods to further eliminate random proton events.

The momentum resolutions of the Hall A HRS is 2.5×10^{-4} (FWHM), the horizontal angular resolution is 2.0 mrad (FWHM), vertical angular resolution is 6.0 mrad (FWHM), and transverse target position resolution is 2.0 mm (FWHM) [18]. With direct vacuum coupling between the scattering chamber and the spectrometer, improvements on HRS resolutions are expected. An optics calibration run is planned, sieve slit data from multiple carbon foil targets will be taken to check angle reconstructions and interaction point reconstructions. Consistency of interaction point reconstructed from the two spectrometers will reject accidental events by more than a factor of 10. Since the beam transverse position can also be determined event-by-event (to 250μm), a requirement on the consistency of the beam transverse position and the reconstructed interaction point from HRS will further reduce the signal to noise ratio.

Coincident time resolution

The current coincident flight time resolution in Hall A is about 2.0 ns FWHM. The resolution is limited by the thin scintillators and phototube timing. In comparison, flight time resolution of 500 ps (FWHM) is routinely obtained in Hall-C coincidence experiments [19]. A detailed Hall A plan of upgrading the trigger scintillators exists which follows the scheme of the Hall C design. The scintillator material and the new phototubes for the upgrade already exist. The upgrade will be a collective Hall A collaboration effort which will benefit any coincident experiment. By the time this experiment could be scheduled, the Hall A time resolution is expected to be 350 ps (FWHM) for each arm, and the 2.0 ns beam structure should be clearly visible.

The coincidence time between the beam RF signal (< 100 ps FWHM) and each of the spectrometers (350 ps FWHM) can provide an ultimate timing resolution of 365 ps (FWHM). Although we do not make the assumption in this proposal, if it happens that Hall B or Hall C is not operating for any reason, two or three beam micro-pulses could be delivered to Hall A every 2.0 ns [20]. This option could further improve our signal-to-noise ratio by a factor of two or three.

Target cell and scattering chamber

Although the current Hall A cryogenic target system has been used in many experiments, the target cell geometry (15 cm long 2.55" diameter with 0.007" Aluminum side wall) is not designed for a measurement demanding high missing mass resolution. Approved experiment E01-104 is planning to build a set of new target cells to minimize energy loss and multiple scattering [21]. A 10.0 cm long, 1.0 cm diameter cell with 10 μm Havar side walls and entrance/exit window will be used in E01-104. We assume a 6.0 cm cell can be made and added to the target loop. A dummy cell is also needed for background measurement. We would like to run at the maximum current allowed in Hall A (100 μA), and a regular raster size of 2×2 mm will be required. The effects of beam heating are not a concern for this experiment since we don't need to measure absolute cross sections.

The standard Hall A scattering chamber will be needed, however, direct vacuum coupling to the spectrometers will be a better choice. The removal of the 16 mil Aluminum scattering chamber window, the 25 cm air gap, and the 7 mil Kapton window at the spectrometer entrance will reduce multiple scattering by 1.5 mrad (FWHM) and reduce y_{target} smearing by 1.0 mm (FWHM) on each spectrometer for this experiment. The approved experiments E01-104 and E94-107 [22] are planning to use vacuum coupling between the scattering chamber and the spectrometer entrances in order to improve resolution. We would also like to install vacuum adapter pieces similar to the design of E01-104. Since the spectrometers will not be moved throughout this experiment, two vacuum adapter pieces will be needed, and the cost will be about $5000 each. All safety regulations applied for E01-104 will be followed.

2.3 Rate Estimate and Accidental Background

According to the test run, with 100 μA beam and the improved target cell design, we expect the raw singles trigger rate on each arm to be around 80-100 kHz. In the electron-arm, the raw e/π^- ratio is about 1:2, and in the hadron-arm, the raw p/π^+ ratio is about 1:2. For a coincident window of 100 ns, the total accidental rate will be about 1 kHz, not enough to cause any serious DAQ dead time. After the PID cuts and the vertex cuts, the effective accidental rate will be about 25 Hz within the 100 ns time window. The real coincident rate is about 2.5 Hz, therefore, within a time-of-flight cut of 2.0 ns the expected signal-to-noise ratio is about 5:1.

2.4 Missing mass resolution

A detailed Monte Carlo study was carried out to address the issue of missing mass resolution. The beam energy spread was taken as 5.0×10^{-5} (FWHM) which has been routinely achieved for Hall A beam delivery. Considerations of target material effects, according to the new target cell design, as well as internal and external bremsstrahlung effects were taken into account. Realistic spectrometer models were used in the simulation to reproduce the acceptances. Improved resolution associated with direct vacuum coupled HRS spectrometer were also considered. Uncertainties of momentum reconstruction from each arm contribute about 0.200 MeV (FWHM) to the missing mass resolution, uncertainties in angle and position reconstruction from each arm contribute about 0.250 MeV (FWHM), beam energy spread contribute about 0.100 MeV (FWHM)[23]. The results of the Monte Carlo simulation are shown in Fig. 8 for Kin-A. A missing mass resolution of 0.5 MeV (FWHM) can be achieved. This resolution is almost a factor of two worse compared to what is expected to be achieved in the hypernuclear spectroscopy experiment E94-107[22] (0.280 MeV).

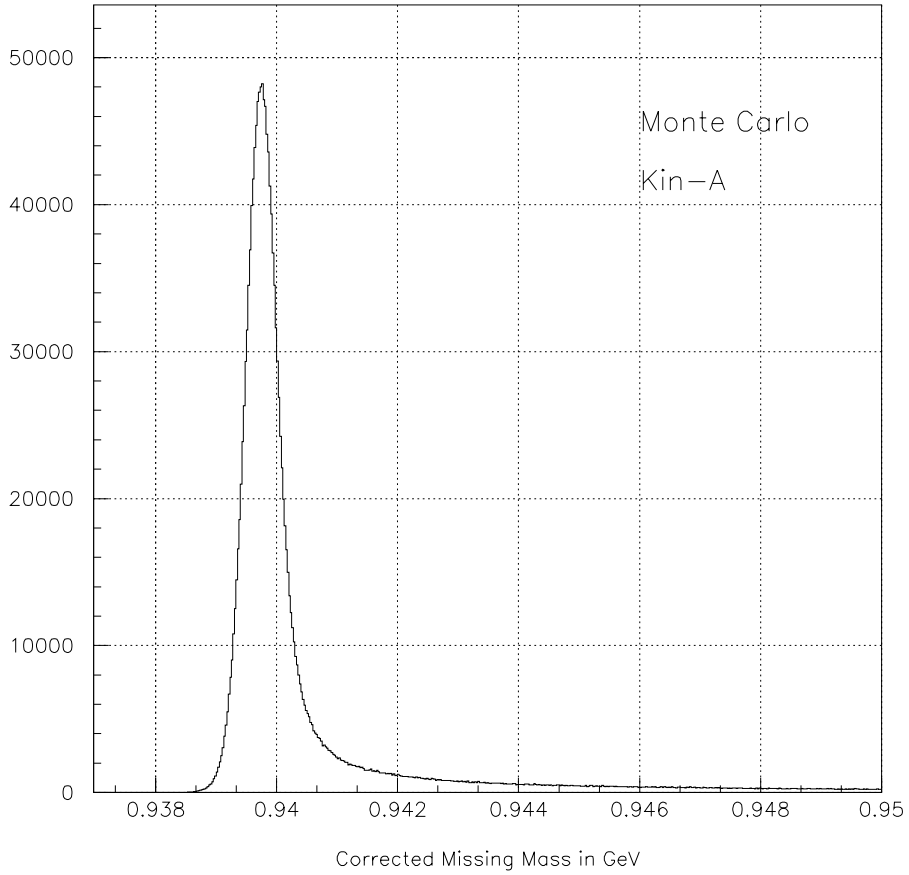

Figure 8: Monte Carlo simulations of Kin-A, a missing mass resolution of about 0.5 MeV is expected after energy loss corrections are applied.

2.5 Results of a test run

We conducted a one-shift test run in April of 2001 to provide guidance for this proposal. The kinematics of the test run was similar to that listed in Table-1 except that the electron arm was set at 19.0° instead of 23.5°, and its momentum was set at 1.040 Gev/c instead of 0.990 GeV/c. The time-of-flight resolution was 2.0 ns (FWHM) after corrections were made for TDC-offsets, time-walk, and particle travel time differences. As shown in Fig. 9, the beam structure was visible but beam pulses were not clearly separated from each other. This time resolution restricted us to run at 33 μA beam in order to keep the signal-to-noise ratio at 1:1. With the planned Hall A scintillator upgrade, a timing resolution better than 365 ps (FWHM) can be achieved.

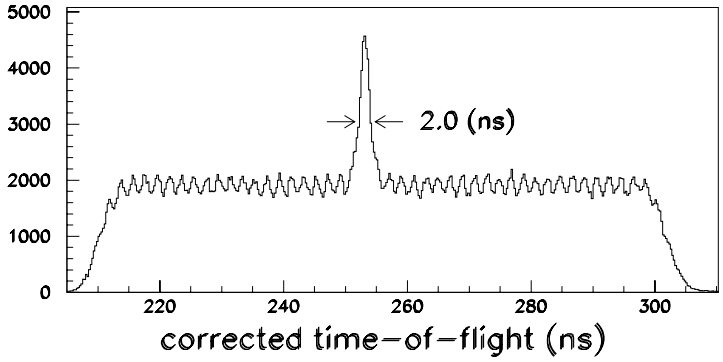

Figure 9: The time-of-flight spectrum in the test run. An improved timing resolution of better than 0.5 ns can be achieved with the planned Hall A scintillator upgrade.

In the test run, a 15 cm long LH2 target cell was used. It had a diameter of 2.55" and had an Aluminum side wall of 0.007" thick. The charge-normalized yield is plotted as a function of reconstructed missing mass in Fig. 10(b). The missing mass resolution was 2.0 MeV (FWHM) for the $p(e,e'\pi^+)n$ calibration of Kin-A. A third power polynomial function fits smoothly through the data, and the fit residues are normalized by the $p(e,e'\pi^+)n$ peak-height as shown in Fig. 10(c). In the mass region of $0.97 < M_{X^0} < 1.06$ GeV, we conclude that

$$K_S \equiv \frac{\sigma_{p(e,e'\pi^+)X^0}}{\sigma_{p(e,e'\pi^+)n}} \leq 10^{-3} \tag{8}$$

3 Source of background and false peaks

3.1 Instrumentation flaws

False shapes can be introduced to the missing mass spectra by instrumentation flaws such as VDC hot wires and local detector inefficiencies. However, in a coincidence experiment, the missing mass is reconstructed combining information from both arms, local inefficiencies on one arm alone can not generate narrow structures. Even

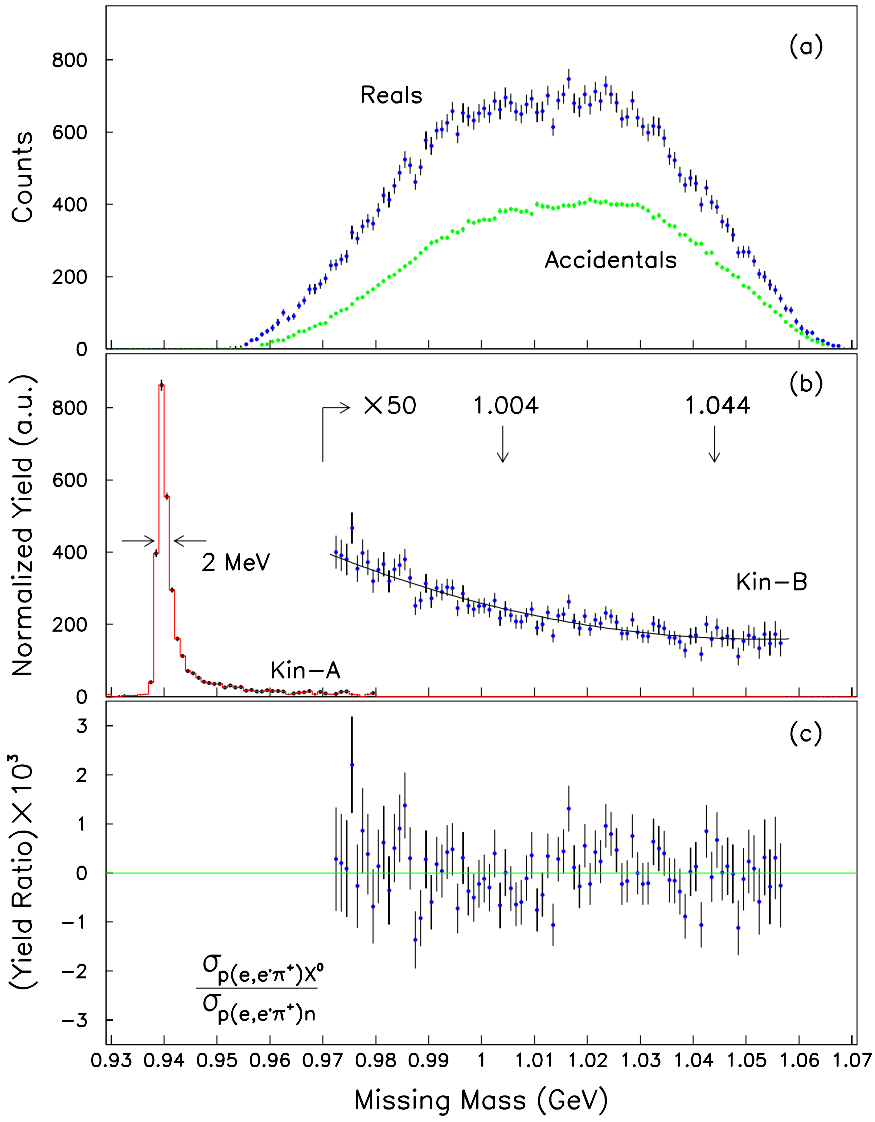

Figure 10: Results from the test run. The reconstructed missing mass spectrum of raw counts is plotted in (a). Charge-normalized $(e, e'\pi^+)$ yields in arbitrary unit are plotted in 1.0 MeV bins in (b). Corrections were made for the effects of pion decay, DAQ dead time, and phase space volumes. A third power polynomial fits the data, the fit residues normalized to the $p(e, e'\pi^+)n$ peak-height are shown in (c). Error bars are statistical only.

if a false peak is created, it should exist in both coincidence events and accidental events. Moreover, singles events in each arm can be used to clearly identify local inefficiencies. Also to our benefit, the wires inside the VDCs are oriented at 45° relative to the dispersion direction, and 4-6 drift-cell hits are normally required for a valid track. This arrangement makes it impossible for hot wires to generate narrow structures along the dispersion direction. We also plan to collect data with slightly altered magnet settings such that false peaks caused by instrumentation flaws will move around in the missing mass spectra.

3.2 Target cell contributions

The thin target entrance/exit windows contribute about $1-2\%$ of total target nucleons. Events from these windows can be clearly identified by interaction point reconstruction. A tight software cut can be introduced to eliminate these events. The target is designed with enough clearance that a well tuned beam should not hit the target side wall in the experiment. The beam position will be measured to 250μm event-by-event, and further software cuts can be introduced on the beam position to eliminate possible beam halo events. In addition, we also plan to take empty cell runs to measure the cell wall contributions.

3.3 Direct μ^+ events and π^+ decays

Since we do not have positive PID for π^+ and μ^+ separation in the hadron arm, direct μ^+ events will be a source of contamination. However, at our kinematic setting, direct $e-\mu^+$ coincident events will have a flight time difference of 1.0 ns compared to that of the $e-\pi^+$ events. With the improved timing resolution, to the first order, we could eliminate $e-\mu^+$ events by a tight flight-time cut. We should also point out that direct μ^+ contamination could only come from $\mu^+\mu^-$ pair productions in which a μ^- would carry considerable momentum in the final state. In the process such as $ep \rightarrow e\mu^+(\mu^- p)$, the continuous momentum distribution in the $\mu^- p$ system would not to generate narrow structures.

A primary pion from the coincident $p(e,e'\pi^+)n$ reaction, with momentum of $\approx$ 0.660 GeV/c, could decay inside the magnet through the $\pi^+ \rightarrow \mu^+\nu_\mu$ reaction and generate a μ^+ along its path. These type of events could in principle be misidentified as $(e,e'\pi^+)$ events with wrong missing masses assigned. However, in order to be traced back to the original interaction points, these μ^+ events have to preserve the direction of the original π^+. Only about 4.0% of the decay μ^+ will stay within a 2.0 mrad cone of the original π^+ direction. In addition, since the decay process happens randomly along the π^+ path in the magnet, it is unlikely to have narrow structures generated in the missing mass. Moreover, at Kin-B setting (with hadron arm at 0.550 GeV/c), the primary pions (at $\approx$ 0.660 GeV/c) have to bounce off the magnet pole face and travel through an irregular flight path even if their decay products can manage to reach the focal plane.

3.4 Pion secondary scattering

In principle, primary pions from the $p(e,e'\pi^+)n$ reaction could undergo a secondary scatter inside the target and acquire lower momenta to form a false peak in the missing mass spectra. However, with the new target cell design, the effective material thickness along the pion's path is only 0.06 g/cm^2 or about 0.1% in nuclear interaction length, thin enough to avoid significant secondary scattering.

3.5 Scattering at the collimator and magnet pole tips

Particles scattered from the spectrometer collimator or magnet pole tips unlikely to be traced back to their vertex point. Additional scattering at the magnet pole tips would also result in extra path length traveled by a particle to push the event off the coincidence timing peak. Software cuts of different collimator size can be applied such that false peaks can be identified.

4 Expected result

4.1 Summary of planned improvements

We summarize the planned improvements for this proposal in Table 2. The new cell geometry reduces the average material thickness from 0.94% r.l. to 0.36% r.l. for the incoming electron, and from 0.90% r.l. to 0.16% r.l. for the scattered electron.

Table 2: Comparison of the test run conditions with this proposal.

Items	Test run	This proposal
Time-of-flight resolution (FWHM)	2.0 ns	< 0.5 ns
Electron arm angle	19.0°	23.5°
Target length (cm)	15.0	6.0
Target diameter (cm)	6.5	1.0
Target wall	7.0 mil AL	1.0 mil Havar
Scattering chamber window	16.0 mil AL	vacuum
Spectrometer entrance window	7.0 mil Kapton	vacuum
Missing mass resolution (FWHM in MeV)	2.0	0.5
Beam current (μA)	33.0	100.0
Beam time (hours)	8	110

4.2 Expected results

This experiment will be able to achieve a missing mass resolution of 0.5 MeV (FWHM) in $p(e,e'\pi^+)X^0$ measurements. Compared with the test run, with shorter target, slightly larger electron arm angle, the lower singles rates plus the improved

timing and vertex reconstruction resolution will allow us to run at a beam current of 100 μA. We expect to collect about 5400 true $(e, e'\pi^+)$ coincidence events within each 0.5 MeV missing mass bin. A null result is shown in Fig 11, and a signal of 1.0×10^{-4} result is shown in Fig. 12. Thus a null results will yield a tight bound of $\sigma_{p(e,e'\pi^+)X^0}/\sigma_{p(e,e'\pi^+)n} \leq 10^{-4}$.

5 Relation with other Jefferson Lab experiment

We have carefully analyzed existing Hall B and Hall C data on the same reaction, and conclude that we cannot obtain a significant result from the existing data. Figure 13 shows a missing mass plot of Hall C E93021 data [24]. Although the kinematics coverage of E93021 allowed some data to be recorded in the missing mass region of our interest, due to the choice of relatively high Q^2, the missing mass resolution is 7.0 MeV (FWHM) and the statistical precision was not high enough to extract meaningful information about a narrow baryon resonances.

Data from Hall B certainly have enough statistics, but the resolution of CLAS is not adequate in the search of narrow resonances, as shown in Fig. 14.

We have also considered the option of a tagged-photon experiment in Hall B and conclude that the energy resolution is not optimized for a search of narrow states. Figure 15 shows a typical missing mass spectra of Hall B g1 data for the reaction of $\gamma p \to \pi^+ X$, a resolution of 16.3 MeV (FWHM) was achieved [25].

6 Summary and Beam Time Request

The beam request is listed in Table 3. Other than the 110 hours of narrow baryon search, two hours of $p(e, e'\pi^+)n$ calibration run is planned. A three hour spectrometer optics run and five hour dummy target run are also planned.

Table 3: Beam time request.

Items	Time (hours)
Beam on LH2 target	112.0
Beam on dummy target	5.0
Spectrometer optics check	3.0
Total	**120.0**

In conclusion, we would like to request 120 hours (5 days) of beam time to verify an experimental claim which is too important to ignore. With the new generation of

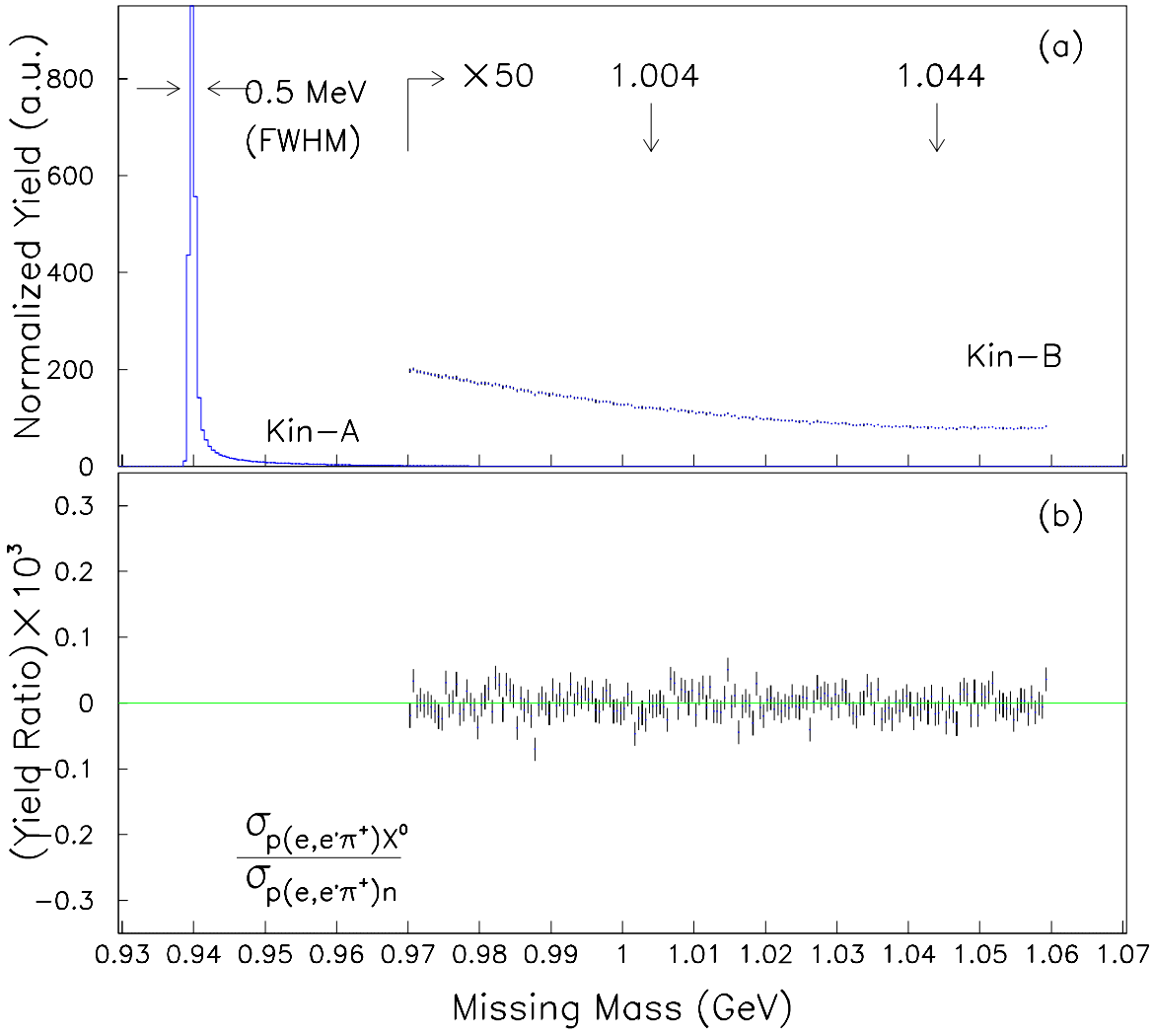

Figure 11: Expected results of charge normalized yield of Kin-B (a), bin size is 0.5 MeV. A 0.5 MeV wide (FWHM) peak from the Monte Carlo is illustrated on the left with the expected yield of Kin-A. The fit residues normalized to the $p(e, e'\pi^+)n$ peak-height are shown in (b) with expected statistical uncertainties.

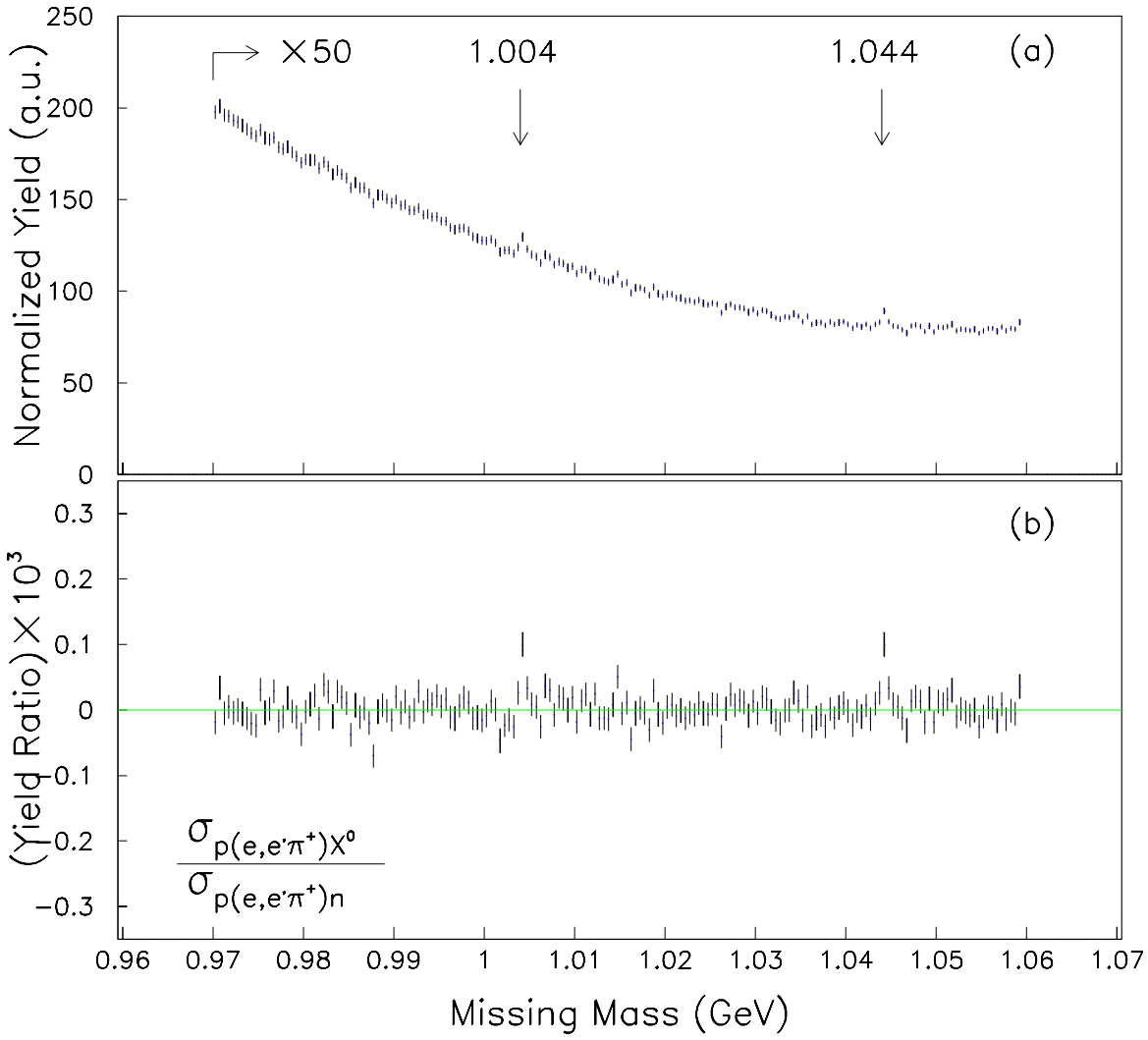

Figure 12: Expected results with resonance signals of $\sigma_{p(e,e'\pi^+)X^0}/\sigma_{p(e,e'\pi^+)n} = 1.0 \times 10^{-4}$ at 1004 MeV and at 1044 MeV. Charge normalized yield is shown in (a) with in same scale as in the previous plot. The fit residues normalized to the $p(e,e'\pi^+)n$ peak-height are shown in (b) with expected statistical uncertainties.

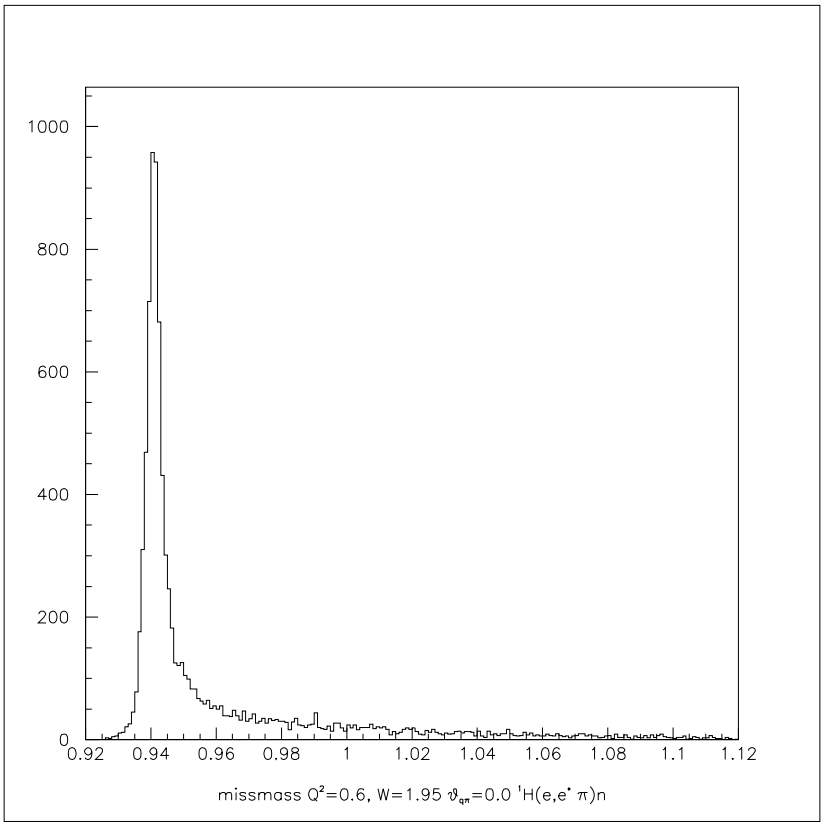

Figure 13: Typical raw missing mass plots of $ep \to e'\pi^+X$ from Hall-C E93021 data.

high resolution spectrometers and the high intensity CW electron beam of Jefferson Lab, a carefully planned experiment could have the opportunity to discover narrow baryon structures which might have been overlooked in all earlier lower resolution experiments. With the planned Hall A scintillator timing upgrade, a well designed target and direct vacuum couplings to the spectrometers, our dedicated search with a 0.5 MeV missing mass resolution could set a tight upper limit of $K_S \leq 1.0 \times 10^{-4}$ on the existence of narrow baryon resonances, and provide a clear confirmation or contradiction of the Saturne experiment. We seriously ask the question: "Is there any neutral baryon resonance exist below pion threshold? or how well do we know there isn't any?"

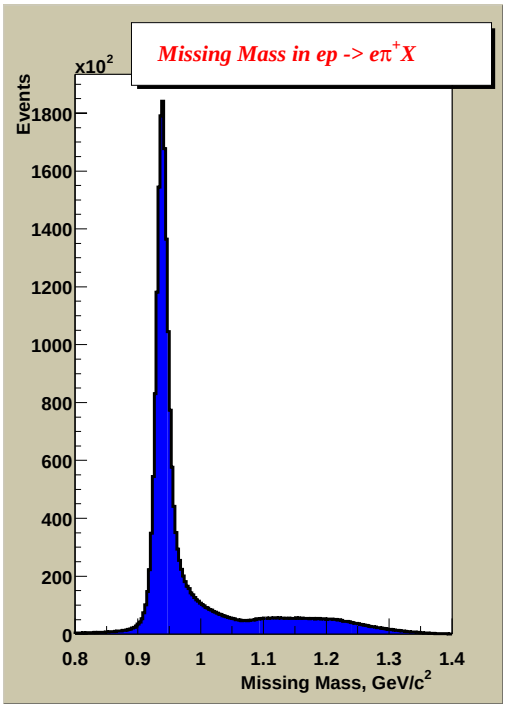

Figure 14: Typical raw missing mass plots of $ep \to e'\pi^+X$ from Hall B data. Beam energy was 1.50GeV, the field setting is at 50% of the full field. No cut on W or Q^2 was applied. The missing mass resolution (FWHM) is 23.8 MeV.

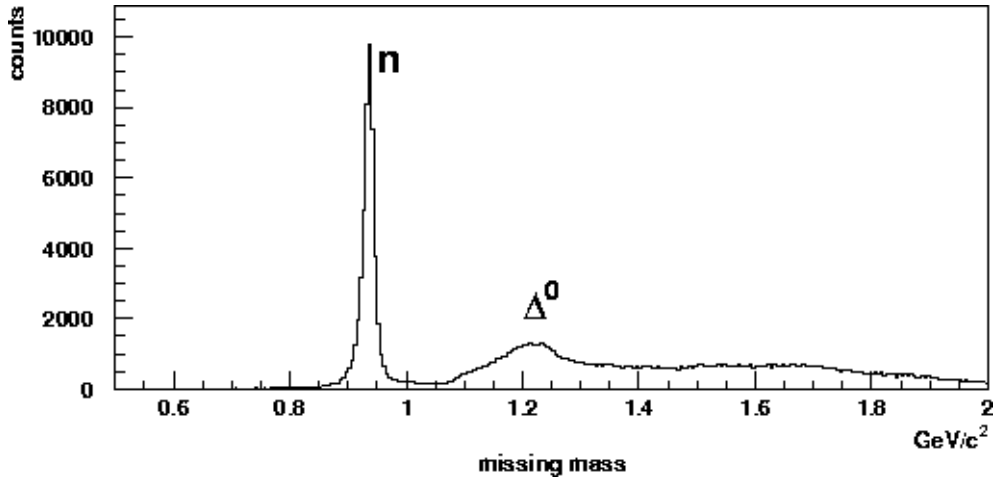

Figure 15: Missing mass spectrum of $\gamma p \to \pi^+X$ reaction from Hall B g1 data.

References

1. R. P. Feynman, *Photon-Hadron Interaction*, (Benjamin New York, 1972).
2. F. Close, *An Introduction to Quarks and Partons*, (Academic Press, N.Y. 1979).
3. S. Ram *et al.*, *Phys. Rev.* D **49**, 3120 (1994).
4. T. T. Nakamura *et al.*, *Phys. Rev.* D **39**, 1261 (1989).
5. B. Tatischeff *et al.*, *Phys. Rev. Lett.* **79**, 601 (1997).
6. Ya. I. Azimov, *Phys. Lett.* B **32**, 499 (1970).
7. L. Masperi and G. Violini, Mod. Phys. Lett. **5**, 101 (1990).
8. A. I. L'vov and R. L. Workman, *Phys. Rev. Lett.* **81**, 1346 (1998).
9. For example in F. J. Federspiel *et al.*, *Phys. Rev. Lett.* **67**, 1151 (1991); and B. E. MacGibbon *et al.*, *Phys. Rev.* C **52**, 2097 (1995).
10. B. Tatischeff *et al.*, *Phys. Rev. Lett.* **81**, 1347 (1998).
11. L. V. Fil'kov, V. L.Kashevarov, E. S. Konobeevskiy *et al.*,hep-ex/0006029, nucl-th/0009044 and nucl-th/0101021, and their earlier work in *Phys. Rev.* C **61**, 044004 (2000).
12. P. Mulders, A. T. Aerts, and J. J. de Swart, *Phys. Rev.* D **21**, 2563 (1980); *Phys. Rev.* D **19**, 2635 (1979); *Phys. Rev. Lett.* **40**, 1543 (1978).
13. N. Konno, *Nuovo Cimento* A **111**, 1393 (1998).
14. Y. Uehara, N. Konno, H. Nakamura and H. Noya, *Nucl. Phys.* A **606**, 357 (1996).
15. K. Konno and H. Nakamura, *Lett. Nuovo Cimento*, **34** 313 (1982);
    K. Konno, H. Nakamura and H. Noya, *Phys. Rev.* D **35**, 239 (1987)
16. A. P. Kobushkin, nucl-th/9804069
17. T. Walcher, hep-ph/0111279 (Nov. 22, 2001).
18. N. Liyanage, Ph.D. thesis, Massachusetts Institute of Technology, (1999).
19. C. Armstrong, Ph.D. thesis, College of William and Marry, (1998).
20. Hari Areti, private communications.
21. E01-104 Hall-A proposal, *Precision Measurement of Electroproduction of π^0 near Threshold*, J. Annand, D. Higinbotham, R. Lindgren, V. Nelyubin spokespersons.
22. E94-107 Hall-A proposal, *High Resolution 1p Shell Hypernuclear Spectroscopy*, S. Frullani, F. Garibaldi, J. LeRose, P. Markowitz and T. Saito spokespersons.
23. J. LeRose, private communications.
24. E93-021 Hall-C proposal, *The Charged Pion Form Factor*, D. Mack spokesperson.
25. B. Asavapibhop, Ph.D. thesis, University of Massachusetts at Amherst, (2000).

Evidence for Narrow Baryon Resonances in Inelastic pp Scattering

B. Tatischeff,[1] J. Yonnet,[2] N. Willis,[1] M. Boivin,[2] M. P. Comets,[1] P. Courtat,[1]
R. Gacougnolle,[1] Y. Le Bornec,[1] E. Loireleux,[1] and F. Reide[1]
[1]*Institut de Physique Nucléaire, CNRS/IN2P3, F-91406 Orsay Cedex, France*
[2]*Laboratoire National Saturne, CEA/DSM CNRS/IN2P3, F-91191 Gif-sur-Yvette Cedex, France*
(Received 29 January 1997)

The reaction $pp \to p\pi^+ N$ has been studied at three energies ($T_p = 1520$, 1805, and 2100 MeV) and six angles from 0° up to 17° (laboratory). Several narrow states have been observed in missing mass spectra at 1004, 1044, and 1094 MeV. Their widths are typically 1 order of magnitude smaller than the widths of N^* or Δ. Possible biases are discussed. These masses are in good agreement with those calculated within a simple phenomenological mass formula based on color magnetic interaction between two colored quark clusters. [S0031-9007(97)03686-7]

PACS numbers: 14.20.Gk, 12.40.Yx, 13.75.Cs, 14.20.Pt

The study of exotic hadrons (mesons and baryons) has been ongoing for several years, motivated by the possibility of relating these exotic states to multiquarks, hybrids, or glueballs. The experimental studies can be separated into two classes. The first class concerns studies of exotic mesons mainly, but also in a few cases of exotic baryons, with explicit exotic quantum numbers, or their exotic combinations. The second class of studies concerns low energy, narrow, exotic states with hidden exotic properties (strangeness or color, etc.) [1]. The main observable here is the small width of the observed structures. Even if such narrowness is not a firm signature [2], this is an essential characteristic from an experimental point of view. Some candidates with relatively large masses exist, and have been observed at Protvino, CERN, and Argonne, although the existence of some of them is still a subject of debate. The corresponding masses are above 1000 MeV for mesons and 1950 MeV for baryons. For experimental reasons (resolution and counting rates), nearly all results of low mass, narrow hadrons concern isovector dibaryons which are seen to be concentrated around certain values [3]. A number of authors have observed many candidates for such isovector narrow dibaryons. This mass spectrum agrees surprisingly well with a simple phenomenological mass formula [3] derived for two colored clusters in a diquark-quadriquark assumption inside an MIT (Massachusetts Institute of Technology) bag model. Different theoretical works have been performed on dibaryons. The first approaches within MIT spherical bags [4] have been improved using cloudy bags [5]. In these last calculations, dibaryons were found at masses close to 2.7 GeV. The same authors predict the existence of molecular states [2] in the lower mass region.

The experiment presented below is the study of the $pp \to p\pi^+ N$ reaction. It was carried out using the proton beam at the Saturne Synchrotron and the SPES3 facility [6]. The incident proton energies were 1520, 1805, and 2100 MeV. The measurements were performed at six angles, for each energy, from 0° up to 17° [7]. The cryogenic H_2 target was 393 mg/cm^2 thick. Both particles, p and π^+, were detected in coincidence in the solid angle of 10^{-2} sr ($\Delta\theta = \Delta\phi = \pm 50$ mrd) of the magnetic spectrometer. The broad range of momenta studied by the detection, $600 < pc < 1400$ MeV at $B = 3.07$ T, allowed the simultaneous study of a large range of missing masses ($939 < M_x < 1520$ MeV). The particle trajectories were localized using drift chambers. The trigger consists of four planes of scintillating hodoscopes. Time of flight measurements over a distance of 3 m, in conjunction with energy loss measurements, allow the identification of the detected particles. Events were lost when both trajectories intersected on each plane of the detector. A simulation code describing the detector has been written in order to correct for such inefficiencies. These corrections, normalizing the data by a factor of $\sim$1.25, are smooth functions, except in a narrow range of $p\pi^+$ invariant masses corresponding to particles detected at the same position on the focal plane. Inside such an invariant mass range the data have been removed, since a peak on the correction function makes any eventual structure at the same mass doubtful.

The random coincidences and eventual wrong identification arising from $pp \to ppX$ events have been taken out using a second time of flight between both particles. The total coincidence window, common to all time of flight channels, was ± 2 ns. Since certain events from a $pp \to ppX$ reaction can simulate real $pp \to p\pi^+ X$ events, checks were carried out to ensure that their contribution is small. They are randomly distributed in the two-dimensional plot of invariant mass against missing mass. In a very small number of cases (0.6% of events), the data reduction code makes a wrong assignment between trigger and chamber informations. These events have been removed.

The necessary conditions required for narrow and small structures study were fullfilled in this experiment. These are (i) a good mass resolution; the σ on missing mass increases from 2.5 up to 9.4 MeV for spectrometer angles

varying from 0° up to 17°, (ii) high statistics ($\geq 10^3$ events per channel), (iii) good particle identification, and (iv) studies in different kinematical conditions in order to check the mass stability of eventual narrow structures, from data obtained at different angles and incident energies.

The $p\pi^+$ invariant mass versus the missing mass of events (before normalization) obtained at 1805 MeV, 0.75° is presented in Fig. 1. The limits of the plot correspond to the lower and upper spectrometer acceptance limits of 600 and 1400 MeV/c, respectively. The empty zone corresponds to the points of intersection of two trajectories on focal plane, where the first drift chamber was located. No other empty (intense) line appears which would correspond to the dead (hot) region in this chamber. The neutron peak is clearly seen on the left side of Fig. 1. It corresponds to events produced with a Δ in invariant mass, partly cut when they lie outside the acceptance, and above, heavier Δ and $p\pi^+$ phase space events. The region with a large population of events at $M_x \sim 1220$ MeV, $M_{p\pi^+} \sim 1200$ MeV corresponds to the double delta production, Δ^0 and Δ^{++}, respectively, in missing mass and invariant mass. Some weakly excited vertical lines appear in the region $1000 < M_x < 1100$ MeV.

Figure 2 shows the result of the projection of the previous two-dimensional plot normalized to constant $\Delta p_p \cdot \Delta p_\pi$ and the same data for the three lowest angles at 1520 and 1805 MeV, selected for missing masses larger than 960 MeV, in order to set off the narrow structures. The decrease of the cross sections and the broadening of the resolution explain why the structures vanish at large angles. The weakly excited lines seen in Fig. 1 are clearly identified in Fig. 2. Empty target measurements have been performed for the same number of incident protons. A low level count rate (<5%) and a flat distribution (without structure) have been observed for the empty target runs.

A careful study has been undertaken in order to make sure that the structures were not produced by events from the $pp \rightarrow p\pi^+ n$ reaction, with the p or π^+ emitted at large vertical angles, which fall outside the useful solid angle acceptance. This could arise for events having a momentum larger than 1400 MeV/c, then slowed down by the lead slits and stainless steel rings at the entrance of the spectrometer. Such an eventuality has been introduced in the simulation code, and shows a small, smooth contribution up to 1060 MeV with a peak arising at masses above and broader than the observed structures. At the missing mass of 1004 (1044) MeV, where the first (second) structure has been observed, the effect of the slits and stainless steel rings is small and varies monotonically with the mass (see

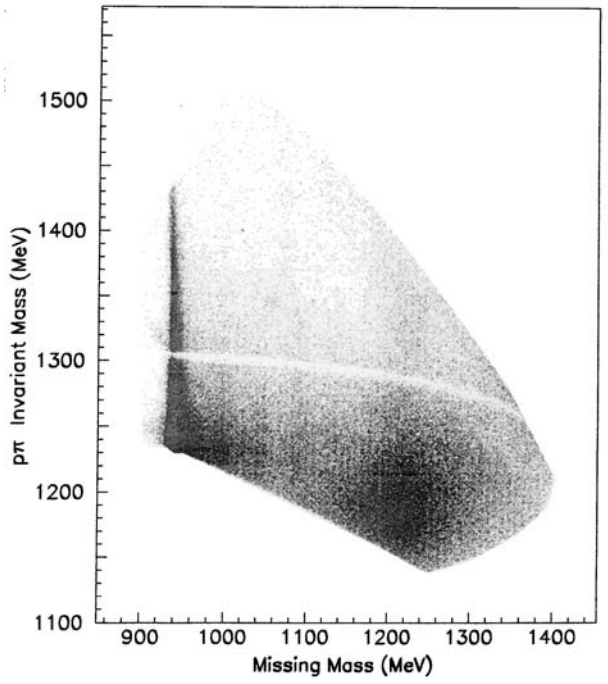

FIG. 1. Two-dimensional plot at 1805 MeV proton energy and 0.75° for the mean value of the two detected particles. The data exhibit clearly the production of delta neutron and two deltas events, and between them an indication of some narrow and small structures.

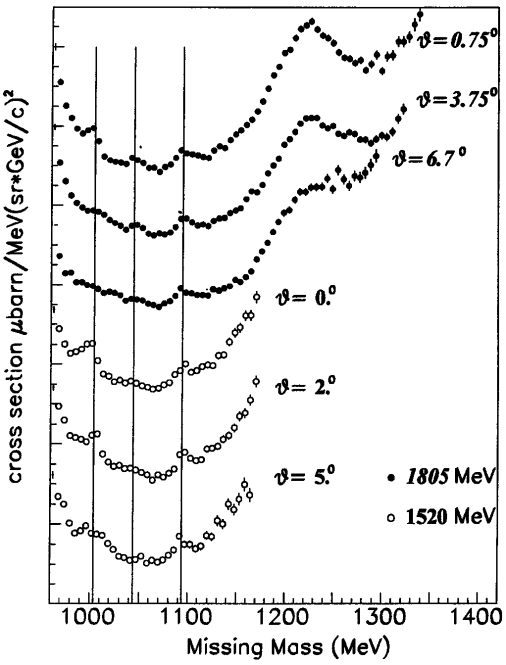

FIG. 2. Missing mass differential cross-sections for the $pp \rightarrow p\pi^+ X$ reaction for the three lowest angles at $T_p = 1520$ and 1805 MeV, selected for missing masses larger than 960 MeV. Data have been binned into 5.6 MeV mass intervals, shifted and amplified in order to allow the presentation of all six angles inside the same figure. Vertical lines indicate the mean position of the structures.

TABLE I. Narrow structure cross sections laboratory in $\mu b/(\mathrm{sr\,GeV}/c)^2$, absolute errors, widths (σ) and number of standard deviations (S.D.).

M_x (MeV)	T_p (MeV)	Angle	Cross sec. (err.)	Width (MeV)	S.D.
1004	1520	0°	271(42)	5	5.9
		2°	260(29)	5	8.6
		5°	223(34)	12	3.6
		17°	observed		
	1805	0.75°	360(29)	6	16.9
		3.75°	120(23)	7	5.1
	2100	0.3°	606(178)	4	2.9
1044	1520	5°	59(27)	4	2
		17°	observed		
	1805	0.75°	144(15)	5	9.1
		3.75°	95(18)	5	5.1
		6.7°	59(14)	8	4.1
		13°	observed		
	2100	0.3°	560(87)	10	6.2
		3°	631(72)	15	6.1
1094	1520	0°	231(44)	7	5
		2°	212(44)	5	4.3
		5°	112(39)	4	2.4
		9°	97(29)	8	3.1
	1805	0.75°	253(20)	8	11.6
		3.75°	261(23)	8	10.6
		6.7°	81(16)	5	4.8
		9°	37(10)	6	3.5
	2100	0.3°	251(49)	7	4.7
		3°	223(45)	7	4.1

[8] for a more detailed discussion). We conclude therefore that there is no contamination in the 1004 and 1044 MeV structures, however, a doubt remains around 1094 MeV.

The cross sections of these structures have been extracted, using polynomial fits for the background and Gaussians for the peaks. The mass structures are well defined, but their cross sections and widths are not well defined. They depend heavily on the shape of the background and on the experimental resolution. Table I summarizes these results. The laboratory cross sections have been normalized to constant momenta ranges. An overall systematic error of 20% can be estimated and is mainly due to the large background subtraction uncertainties.

Although many experiments devoted to various other studies have explored the baryonic excitation function between the nucleon and delta, and have often observed some shoulders or discontinuities in that region, none of them were accurate enough in order to be able to ascertain the real presence of new states. A (not exhaustive) list of such experiments is presented in Table II.

As pointed out before, narrow baryons, which are sometimes still a subject of debate, have already been observed in different laboratories. They appear as candidates for exotic baryons with hidden strangeness in invariant masses of strange baryons and strange mesons [22–25].

Although it is not proven that these structures are a manifestation of colored quark clusters, we have considered such an assumption. The mass formula for two clusters of quarks at the ends of a stretched bag was derived some years ago in terms of color magnetic interactions [4,26];

$$M = M_0 + M_1[i_1(i_1 + 1) + i_2(i_2 + 1) + (1/3)s_1(s_1 + 1) + (1/3)s_2(s_2 + 1)], \quad (1)$$

where M_0 and M_1 are parameters deduced from mesonic and baryonic mass spectra and $i_1(i_2)$ and $s_1(s_2)$ are isospin and spin of the first and second quark cluster, respectively. We make the assumption that the clusters are $q^2 - q$ or $(q\overline{q})^2 - q^3$. The spin (isospin) values for a diquark $(q\overline{q})$ cluster are 0 or 1 and for a three quark cluster $1/2$ or $3/2$. Since the masses correspond to zero radial excitation, all parities are positive.

TABLE II. Experiments having studied the baryonic mass region between nucleon and delta.

Particles	Accelerator	Reaction	Reference
nucleons	LAMPF	$np \to pX$ (0°)	B. E. Bonner *et al.* (1983) [9]
		$pp \to p\pi^+ n$ (800 MeV)	A. D. Hancock *et al.* (1983) [10]
		$pp \to p\pi^+ n$ (800 MeV)	J. Hudomalj-G. *et al.* (1978) [11]
	Saturne	$p(^3\mathrm{He}, t)X$	D. Contardo *et al.* (1986) [12]
		$^3\mathrm{He}(p, t)X$	B. Tatischeff *et al.* (1978) [13]
		$np \to pX$	G. Bizard *et al.* (1976) [14]
photons	MAMI	$\gamma\, p \to \pi^0 X$	M. Fuchs *et al.* (1996) [15]
		$\gamma\, p \to \gamma\, X$ (90°)	C. Molinari *et al.* (1996) [16]
		$\gamma\, p \to p\pi^+\pi^-$	A. Braghieri *et al.* (1995) [17]
		$\gamma\, p \to p\pi^0\pi^0$	"
		$\gamma\, n \to p\pi^+\pi^0$	"
	Saskatchewan	$\gamma\, p \to \gamma X$	E. L. Hallin *et al.* (1993) [18]
	Brookhaven	$\gamma\, p \to \pi^0 X$	G. Blanpied *et al.* (1992) [19]
	Saclay-ALS	$\gamma\, p \to \pi^0 X$	E. Mazzucato *et al.* (1986) [20]
	Bonn	$\gamma\, d \to pX$	J. Arends *et al.* (1996) [21]

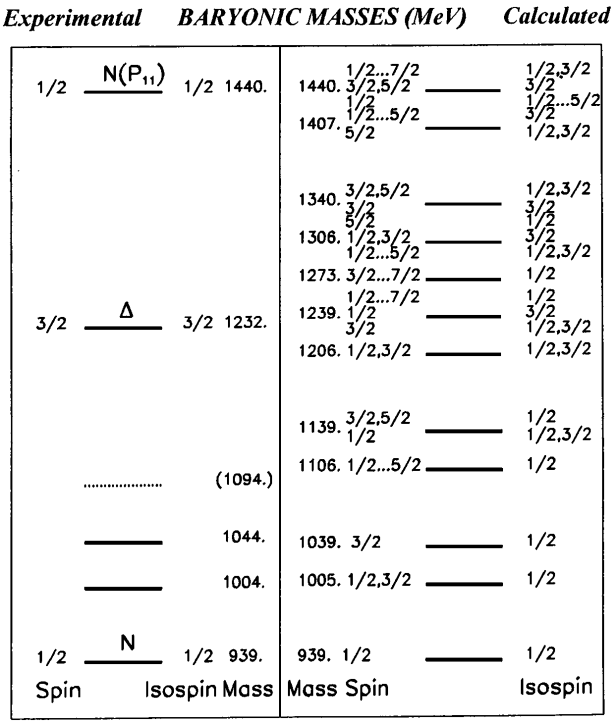

FIG. 3. Baryonic experimental and calculated masses.

In order to define the two parameters, we first assume that the nucleon mass is obtained when $i_1 = s_1 = 0$, and $i_2 = s_2 = 1/2$, giving therefore the nucleon quantum numbers $S = I = 1/2$. We assume also that the Roper resonance at 1440 MeV (the first excited state of the nucleon) is obtained with $i_1 = 1$, $s_1 = 0$, $i_2 = 3/2$, and $s_2 = 1/2$ giving, among degeneracy, possible experimental quantum numbers $S = I = 1/2$. Such assumptions allow us to predict the masses of the two first possible $S = I = 3/2$ states at 1206 ($i_1 = s_1 = 1$ and $i_2 = s_2 = 1/2$) and 1239 MeV ($i_1 = 1$, $s_1 = 0$, $i_2 = 1/2$, and $s_2 = 3/2$), close to the mass of the first delta resonance. Such assumptions determine the values of $M_0 = 838.2$ MeV and $M_1 = 100.3$ MeV. The corresponding mass spectra obtained using relation (1) without any adjustable parameter, is shown in Fig. 3. As in the case of narrow isovector dibaryons [3], a good agreement is observed between the experimental and calculated masses. Masses, spins, and isospins for additional levels are predicted, and often have several possible spin and isospin values due to the degeneracy mentioned above. It is not excluded that more precise experiments will, in the future, observe these levels. Below the pion emission thresholds, 1075 MeV for baryons and 2012 MeV for dibaryons, the only possible decay channel is the radiative one. Below and above the pion emission thresholds, the assumption that they are states of two colored quark clusters gives a good agreement between the color magnetic mass formula and the experimental observations.

In conclusion, three narrow baryonic states have been observed at the following masses: 1004, 1044 MeV, and with a smaller confidence at 1094 MeV, without any anomalous experimental behavior. The latter state is only 19 MeV above the pion threshold mass. The widths of each of these three observed states are probably in the range 4–15 MeV. Such narrow widths are consistent with the need for radiative decay of the two lowest mass structures, and with the small phase space for the strong decay of the third.

[1] L. G. Landsberg, Phys. At. Nucl. **27**, 42 (1994).
[2] E. L. Lomon, in Proceedings of the XIIIth International Seminar on High Energy Physics Problems, Dubna, 1996 (to be published).
[3] B. Tatischeff, in Proceedings of the XIIth International Seminar on High Energy Physics Problems, Dubna, 1994 (to be published).
[4] P. J. Mulders, A. T. Aerts, and J. J. de Swart, Phys. Rev. D **21**, 2653 (1980); Phys. Rev. D **19**, 2635 (1979); Phys. Rev. Lett. **40**, 1543 (1978).
[5] P. LaFrance and E. L. Lomon, Phys. Rev. D **34**, 1341 (1986); P. Gonzalez, P. LaFrance, and E. L. Lomon, Phys. Rev. D **35**, 2142 (1987).
[6] M. P. Comets *et al.*, Report No. IPNO DRE 88-41.
[7] Only three angles at 2100 MeV: 0.7°, 3°, and 9°.
[8] B. Tatischeff and J. Yonnet, in Proceedings of the XIIIth International Seminar on High Energy Physics Problems, Dubna, 1996 (Ref. [2]).
[9] B. E. Bonner *et al.*, Phys. Rev. D **27**, 497 (1983).
[10] A. D. Hancock *et al.*, Phys. Rev. C **27**, 2742 (1983).
[11] J. Hudomalj-Gabitzch *et al.*, Phys. Rev. C **18**, 2666 (1978).
[12] D. Contardo *et al.*, Phys. Lett. **168B**, 331 (1986).
[13] B. Tatischeff *et al.*, Phys. Lett. **77B**, 254 (1978).
[14] G. Bizard *et al.*, Nucl. Phys. **B108**, 189 (1976).
[15] M. Fuchs *et al.*, Phys. Lett. B **368**, 20 (1996); V. Bernard, N. Kaiser, and Ulf-G. Meissner, Phys. Lett. **B378**, 337 (1996).
[16] C. Molinari *et al.*, Phys. Lett. B **371**, 181 (1996).
[17] A. Braghieri *et al.*, Few-Body Syst. Suppl. **8**, 171 (1995).
[18] E. L. Hallin *et al.*, Phys. Rev. C **48**, 1497 (1993).
[19] G. Blanpied *et al.*, Phys. Rev. Lett. **69**, 1880 (1992).
[20] E. Mazzucato *et al.*, Phys. Rev. Lett. **57**, 3144 (1986).
[21] J. Arends *et al.*, Nucl. Phys. **A412**, 509 (1984).
[22] S. V. Golovkin *et al.*, Z. Phys. C **68**, 585 (1995); Phys. At. Nucl. **58**, 1342 (1995).
[23] A. N. Aleev *et al.*, Z. Phys. C **25**, 205 (1984).
[24] V. M. Karnaukhov, C. Coca, and V. I. Moroz, Phys. At. Nucl. **58**, 796 (1995).
[25] J. Amirzadeh *et al.*, Phys. Lett. **B89**, 125 (1979).
[26] C. Besliu, L. Popa, and V. Popa, J. Phys. G **18**, 807 (1992).

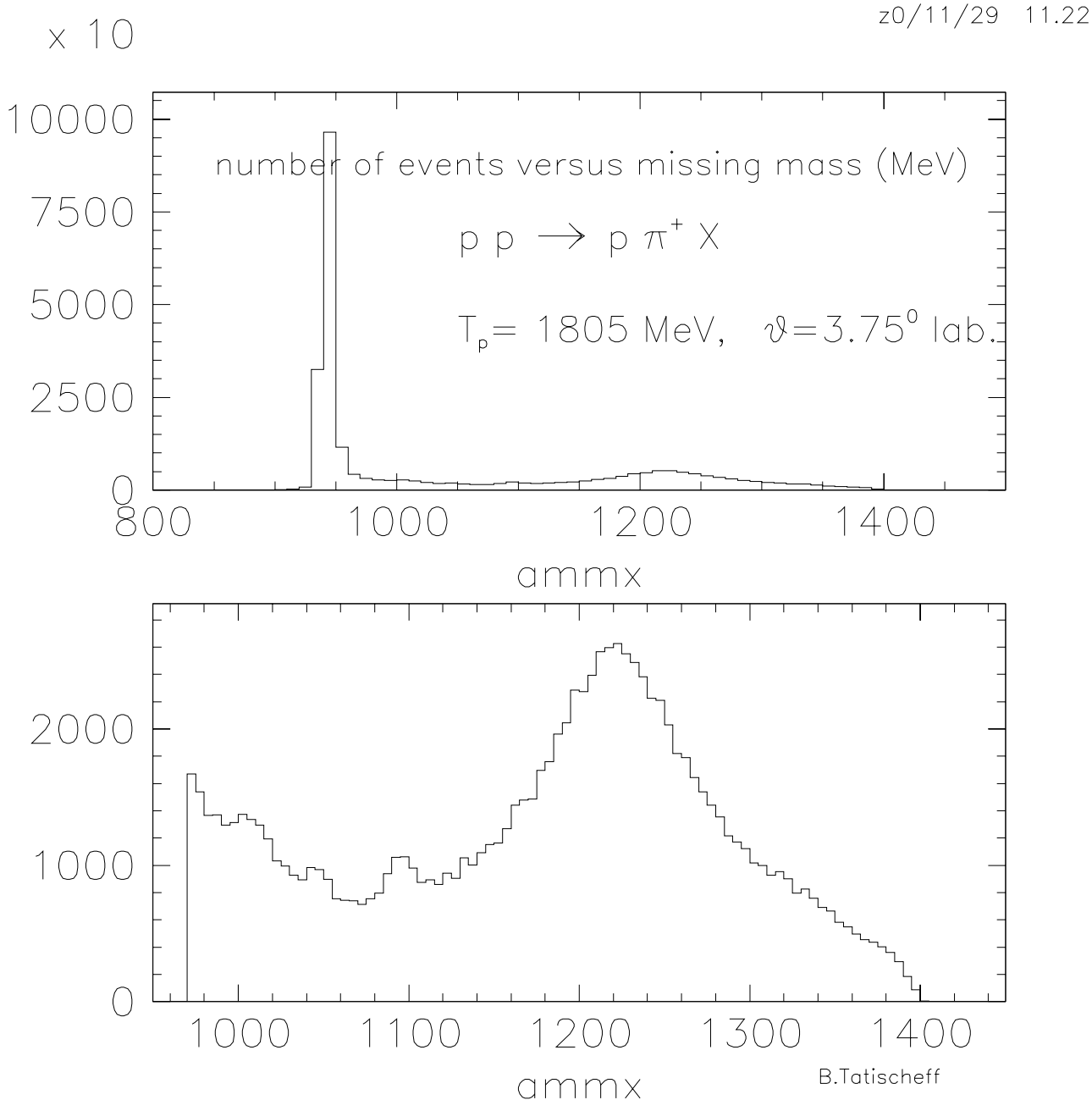

Figure A-1: Raw missing mass plot of $pp \to p\pi^+X$ at $T_p = 1805$ MeV and $\theta_p = 3.75°$ without acceptance correction. The horizontal axis indicates missing mass in MeV. Top plot shows the whole spectrum with a narrow nucleon peak to the left and a broad Δ bump to the right. The bottom plot shows the region above the nucleon mass. (B. Tatischeff, private communications.)

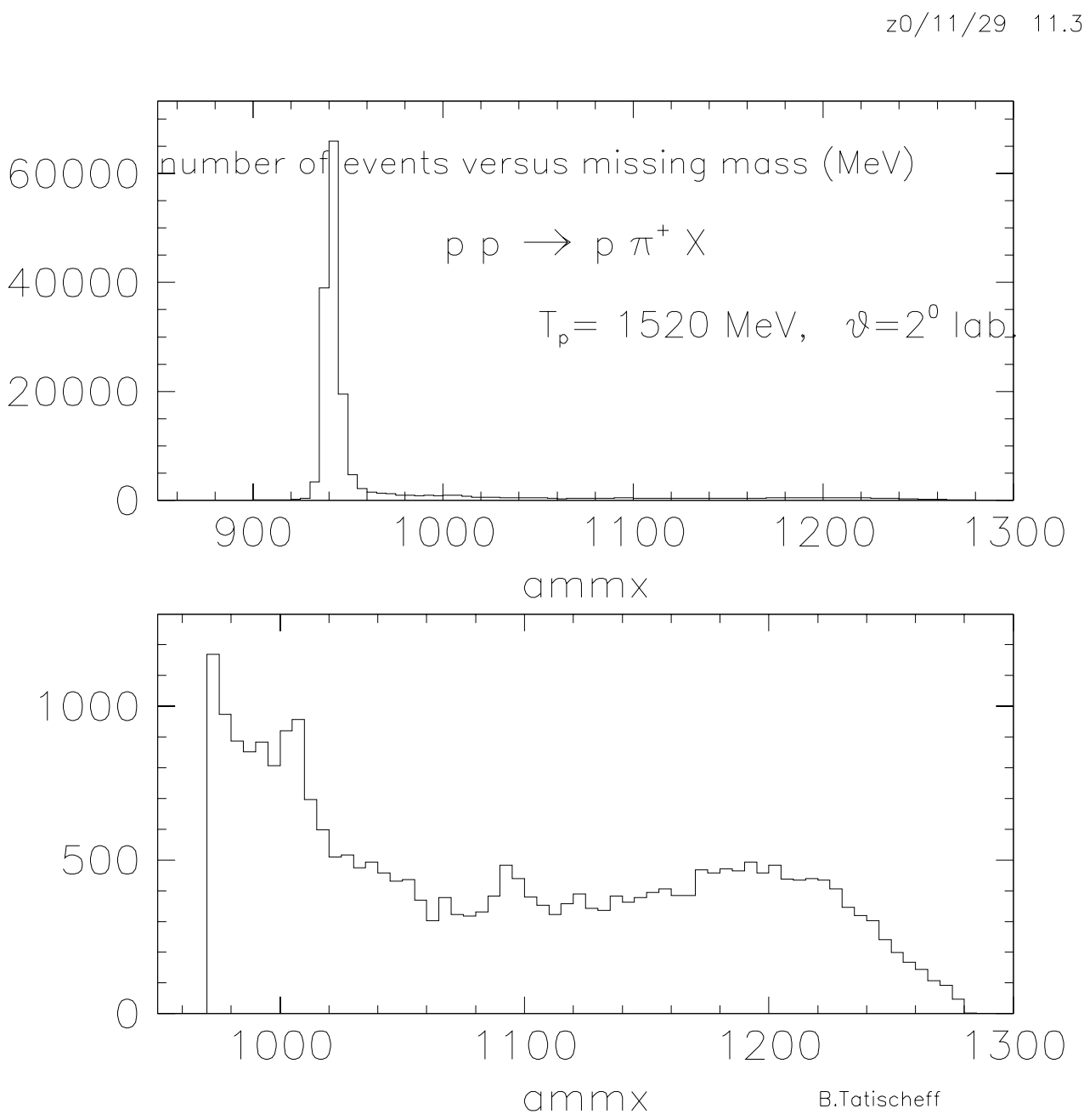

Figure A-2: Raw missing mass plot of $pp \to p\pi^+X$ at $T_p = 1520$ MeV and $\theta_p = 2°$ without acceptance correction. The horizontal axis indicates missing mass in MeV. (B. Tatischeff, private communications.)